

# Design and characteristic evaluation of a novel amphibious spherical robot

Jian Guo<sup>1</sup> · Shuxiang Guo<sup>1,2</sup> · Ligu Li<sup>1</sup>

Received: 21 January 2016 / Accepted: 28 April 2016  
© Springer-Verlag Berlin Heidelberg 2016

**Abstract** This paper presents a new type of amphibious spherical robots. The robot includes four drive units. Each drive unit consists of two servo motors, a water-jet propeller, a DC motor and a wheel. The robot can constitute three movement structure ways according to the environment. When the robot enters water, it adopts water jet propulsion. According to different land conditions, there are two movement patterns to switch. One is a quadruped movement pattern which is available to climb over obstacles; the other is a driving wheel movement pattern which is used to speed up the movement of robot under the flat terrain. Characteristic evaluation experiments on land for a novel amphibious spherical robot were conducted. Underwater motions of the robot mainly rely on the four water-jet propellers, it is necessary to measure relationship between actuating force of the water-jet propeller and the duty ratio. Gambit software is employed to establish and mesh the water-jet propulsion model. Simulation analysis of the models is implemented by FLUENT software. Localization control of the robot and wireless control of the robot were conducted. Finally, experiment results indicated that the developed novel amphibious spherical robot is feasible to develop marine resources and implement marine missions.

## 1 Introduction

At present, underwater vehicles can mainly be included remote operated underwater vehicles (ROVs) and autonomous underwater vehicles (AUVs) (Ting et al. 2012). In recently, researches on autonomous underwater robots have become a hot spot all around the world. A variety of underwater robots have increased dramatically, in that underwater robots have widely applications such as getting submarine sampling, pollution detection, deep-ocean exploration and seabed tracking (Ryuha et al. 2015; Saout and Ananthakrishnan 2011; Marani et al. 2009).

Spherical shape has many excellent properties. Helsinki University of Technology bred the world's first spherical robot named Rollo whose designers are the Halme et al. (1996). Then spherical underwater robots more and more get the welcome of scholars. The University of Manchester developed a Micro-Autonomous Underwater Vehicles which had a diameter of 150 mm and 4 DOF in 2012. DC motor/propeller thruster units were selected as the means of propulsion in both planes (Watson et al. 2012).

MIT developed an egg-shaped underwater robot for infrastructure inspection in 2013. The robot utilized jet propulsion and smooth, spheroidic shapes to achieve multi-DOF manoeuvrability and unique motions such as forward and reverse motions, sway translations, and turning in place. The system dynamics and control literature issues with non-minimum phase behaviour have been explored. In order to move in the water, the small robot used a unique feed mechanism of the propulsion system including six pumps (Mazumdar and Asada 2011, 2013; Mazumdar et al. 2012, 2013). McGill University developed an amphibious robot which can work both on land and in water. A new class of multi-purpose leg is used to for walking and swimming (Dey et al. 2013).

---

✉ Jian Guo  
jianguo@tjut.edu.cn

✉ Shuxiang Guo  
guoshuxiang@hotmail.com

<sup>1</sup> Tianjin Key Laboratory for Control Theory and Application in Complicated Systems and Biomedical Robot Laboratory, Tianjin University of Technology, Tianjin, China

<sup>2</sup> Intelligent Mechanical Systems Engineering Department, Kagawa University, Takamatsu, Japan

Professor Guo et al. at the Kagawa University developed some spherical underwater robots. Robots can be divided into underwater spherical robot (Guo et al. 2010; Lin et al. 2013; Li et al. 2015; Yue et al. 2013a, b, 2015) and amphibious spherical robots (Shi et al. 2013; Guo et al. 2012, 2013; Pan et al. 2015; Li et al. 2015). The characteristics of the water-jet thruster have been analyzed. They focused on the improved propulsion system structure, a hydrodynamic analysis using computational fluid dynamics and improved modeling method for a water-jet based multi-propeller propulsion system. At the same time, a mother-son multi-robot cooperation system was proposed, named GSL system, which could carry some microrobots as son robots. These microrobots can accomplish simple tasks such as avoid obstacle and grasp the small object (Yue et al. 2015a, b; Shi et al. 2011; Guo et al. 2012).

There are also some institutions that are engaged in this field in China, such as Harbin Engineering University and Beijing University of Post and Telecommunications. Harbin Engineering University developed spherical robots based on the principle of vector propulsion. The robot can achieve 3 DOF movements in water (Guo et al. 2011). Beijing University of Post and Telecommunications also developed their own spherical robots (Lan et al. 2010).

Legs and wheels are two widely adopted methods utilized on the ground locomotion. Wheel movement has excellent performance of power efficiency and movement speed, which can hardly be completed by legs. Thus, the study of a leg-wheel hybrid platform more and more get the welcome of scholars. Leg-wheel hybrid platform is suitable for general indoor-outdoor environments.

National Taiwan University developed a leg-wheel hybrid robot Quattroped in 2009. This robot was implemented with a transformation mechanism which directly changes the morphology of wheels (i.e. a full circle) into 2 degree-of-freedom legs (i.e. combining two half-circles as a leg) (Shen et al. 2009). Roller Walker (Endo and Hirose 1999) incorporates a passive wheel on the foot of each 3 DOFs leg. And the locomotion can be switched from quadruped walking into roller skating on the flat ground. But those robots only can work on land.

Based on aforementioned background and relative researches, this paper proposes a new type of amphibious spherical robots. The robot includes four drive units which can constitute three movement structure ways according to the environment, including wheel structure movement or quadruped walking movement adopted on land and water jet propulsion in water. The ground is relatively flat, wheel structure pattern is adopted by the robot to improve movement speed. While the ground is more rigorous, the robot can use quadruped movement pattern to climb over

obstacles. And the paper mainly states characteristic evaluation on land for a novel amphibious spherical robot.

This paper consists of six parts. Section 2 introduces structure design of novel amphibious spherical robot. Then Sect. 3 illustrates two kinds of land movement gait of amphibious spherical robot. A series of land experiments were conducted to analyze kinetic characteristic of the robot, including location experiment of the robot. In Sect. 4, hydrodynamic performance of the Water-jet propeller model was analyzed. In Sect. 5, wireless control experiment of the robot was conducted. Finally, we come to conclusions and bring forward future work in Sect. 6.

## 2 Structure design of the novel amphibious spherical robot

### 2.1 Structure of the novel amphibious spherical robot

The novel amphibious spherical robot mainly consists of a sealed upper hemisphere shell, a plastic circular plate and four drive units. The structure diagram of the robot is shown as Fig. 1. Four drive units are symmetrical installed on the plastic circular plate. Each drive unit includes two servo motors, a water-jet propeller, a DC motor and a wheel. Figure 2 shows the links between various components. The control circuits, sensors and batteries are installed inside the sealed upper hemisphere shell so as to achieve the waterproof effect.

Figures 3 and 4 show the two movement patterns that the novel amphibious spherical robot will adopt according to land status information. Figure 3 indicates the initial gait of quadruped movement. Figure 4 indicates the initial gait of wheel movement. According to land terrain conditions, two kinds of way can switch freely. Switch between the two modes is achieved by controller controlling eight servo motors.

### 2.2 Control and power system

The control system of the spherical robot is shown in Fig. 5. We chose STM32 and Atmega2560 as core controller. Eight channels of PWM signals control eight servo motors. Using eight input/output ports control four water-jet propellers. Using eight input/output ports control four DC motors. The control system also included a NRF905 remote control module, GSM module and GPS. For the energy system, two LI-PO batteries are used. The voltage of the battery is 7.4 V. Battery capacity is 5000 amh. One is used to supply for microcontroller; the other one is used to supply for servo motors, DC motors and water jet propellers.

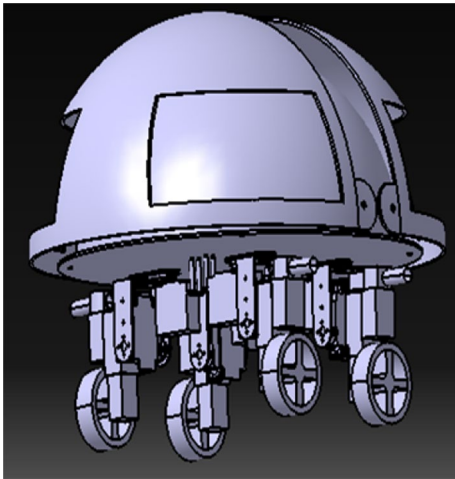


**Fig. 1** The structure of the novel amphibious spherical robot

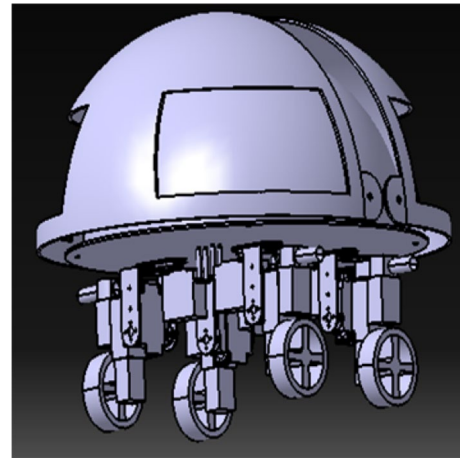


**Fig. 4** Initial gait of wheel movement

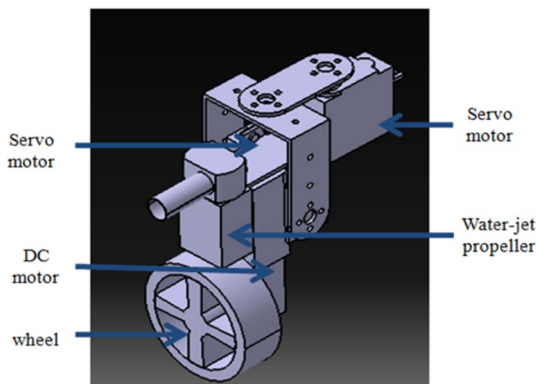


**Fig. 2** The structure of the drive unit

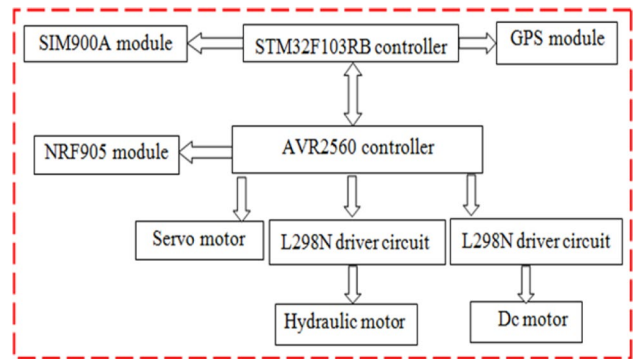


**Fig. 5** Control system

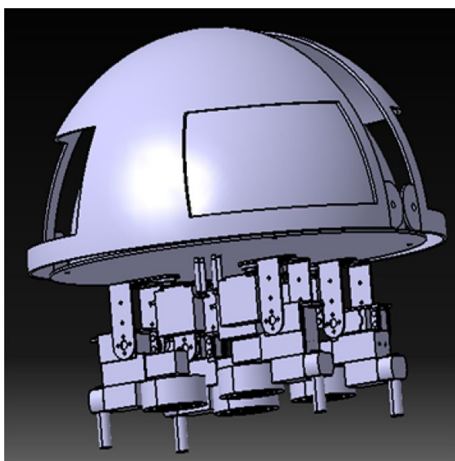


**Fig. 3** Initial gait of quadruped movement

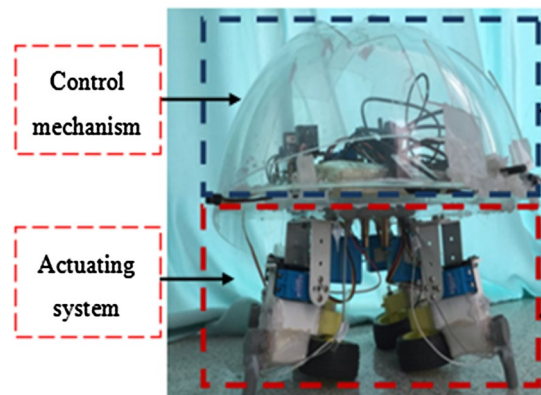


**Fig. 6** Prototype novel amphibious spherical robot

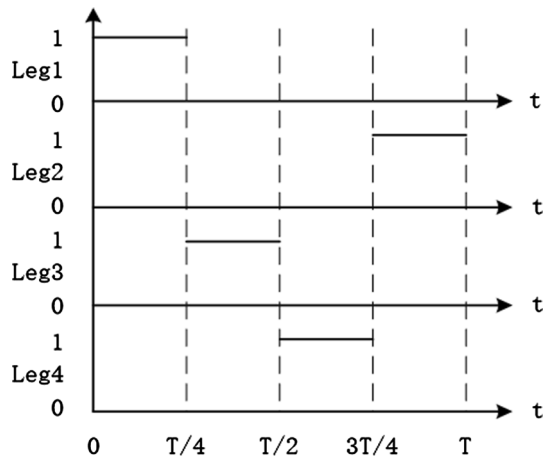


Fig. 7 Crawling gait

### 3 Land movement analysis of amphibious spherical robots

#### 3.1 Prototype of a novel amphibious spherical robot

Figure 6 shows prototype novel amphibious spherical robot. The robot is small in size. Maximum diameter is less than or equal to 40 cm. The robot consists of two parts. The upper part of the robot is control mechanism; the lower part is actuating system. The two servo motors on the same

drive unit are mutually perpendicular. Each drive unit can realize two degrees of freedom movement. We chose to use waterproof servo motor (Fig. 6) produced by Raboesch Company and HS-5646WP Water-jet propeller made by Hitec Company.

#### 3.2 Quadruped movement gait

Nature provides perfect models for robots. When the robot walks on land, the amphibious spherical robot can be regarded as a quadruped robot (Loc et al. 2012; Cai et al. 2013; Kazemi et al. 2013). The nozzle of water-jet propeller is used as the robot's leg. There are four kinds of gaits when quadruped robot move on land, including trotting gait, crawling gait, gallop gait and hoof slipped gait. Considering the system stability and feasibility, the robot in this paper adopts crawling gait to walk on land. Experience results will be analyzed in the next section. Crawling gait is that the robot's four legs walk on the ground in a certain order. From Fig. 7, motion sequence of the robot's legs is leg1, leg3, leg4 and leg2. In Fig. 8, 0 indicates that leg contacts with the ground and 1 indicates that leg departs from the ground. So duty ratio of crawling gait is  $B = 0.75$  in a cycle  $T$ . That is to say, at any one time, there are three legs on the ground; the fourth leg is off the ground. We regard the leg contacting the ground as supporting leg. The leg off the ground is named swing leg (Wan et al. 2014). The

Fig. 8 Crawling movement experiments on different terrains

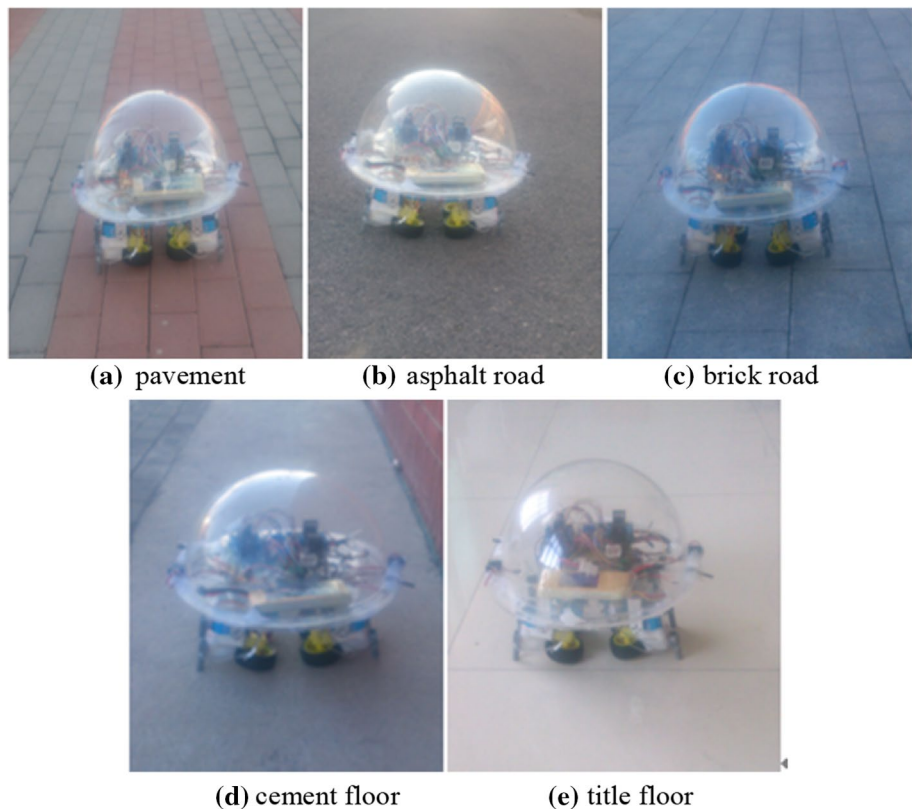
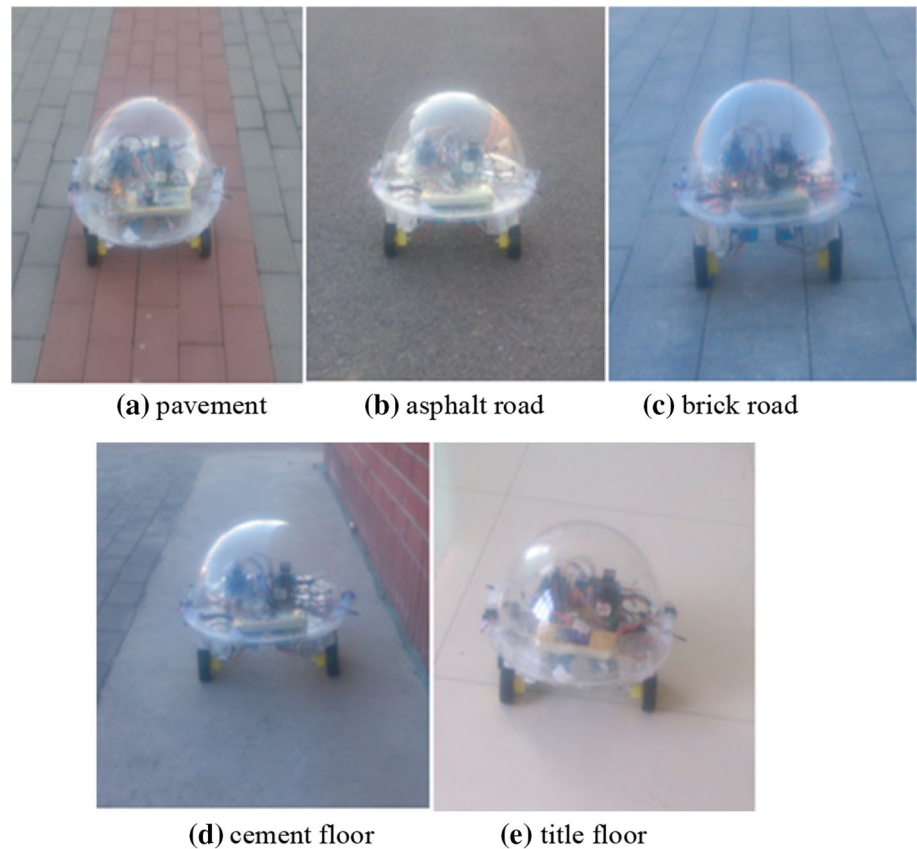


**Fig. 9** Wheel movement experiments on different terrains



preliminary mechanical analysis of an amphibious spherical robot with four legs has been done (He et al. 2015).

### 3.3 Wheel movement gait

Wheel movement is another way that novel amphibious spherical robot can choose. When the ground is flat, the robot can choose this way. Because it can improve movement speed of the robot. Four wheels of the robot are respectively controlled by a DC motor. So it is a system of Four-Wheel-Independent. The movement direction of the robot not only can be controlled by servo motor of each drive unit, but also can be changed by the output of the DC motor rotational speed difference. When conducting land experiment, we set the four wheels running state.

### 3.4 Experiments and results

In order to evaluate characteristics on land for the novel amphibious spherical robot, we conduct many experiments. Based on two movement patterns, Fig. 8 shows experiments of quadruped movement crawling gait were conduct under the condition of different terrains and different loads on land. Figure 9 shows that experiments of wheel movement

gait were conduct under the condition of different terrains and different loads on land. Terrains in the experiments include pavement, asphalt road, brick road, cement floor and tile floor. These terrains can be characterized by different coefficients of friction. Different loads on the robot we choose are respectively 0, 204 and 403 g. Finally, we get the data graph under a variety of terrains.

In order to ensure the effectiveness of the experiment data, all experiments were repeated several times to achieve an average velocity. When the robot walked in crawling gait, the robot was programmed to move straight forward for 1 m. By measuring the time, average velocity was calculated. When the robot walked in wheel movement gait, the robot's movement speed is faster. In order to make accurate measurement, the robot was programmed to move straight forward for 8 ms. By measuring the distance, average velocity was calculated. At last, the experience results of quadruped movement crawling gait are shown as Fig. 10. The experience results of wheel movement gait are shown as Fig. 11.

When the novel amphibious spherical robot walked in quadruped movement crawling gait, we can get the relationship figure between the frequency and speed of the robot. It is shown in Fig. 10.

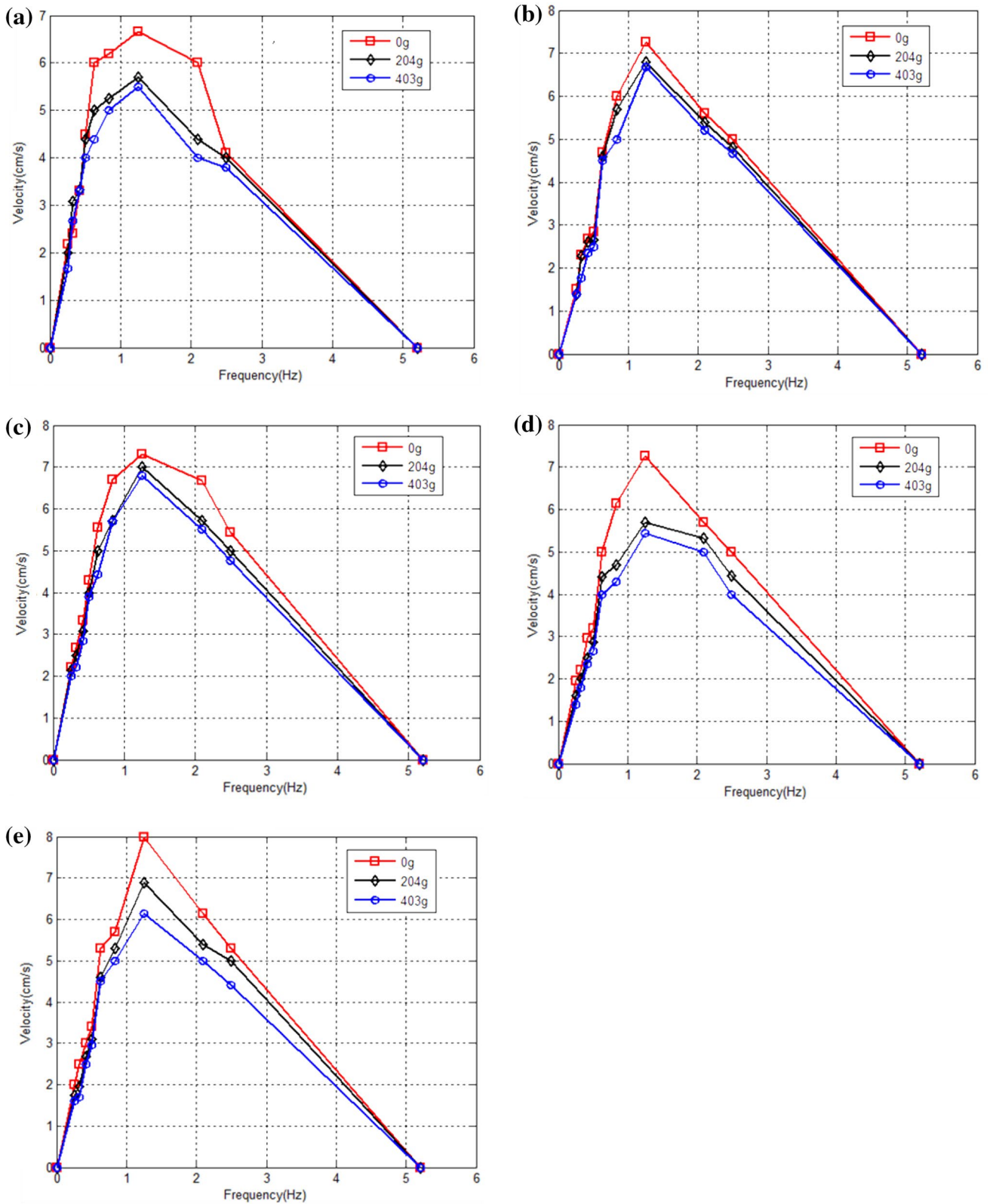


**Fig. 10** Results of crawling movement experiments on different terrains: **a** pavement, **b** asphalt road, **c** brick road, **d** cement floor, and **e** tile floor

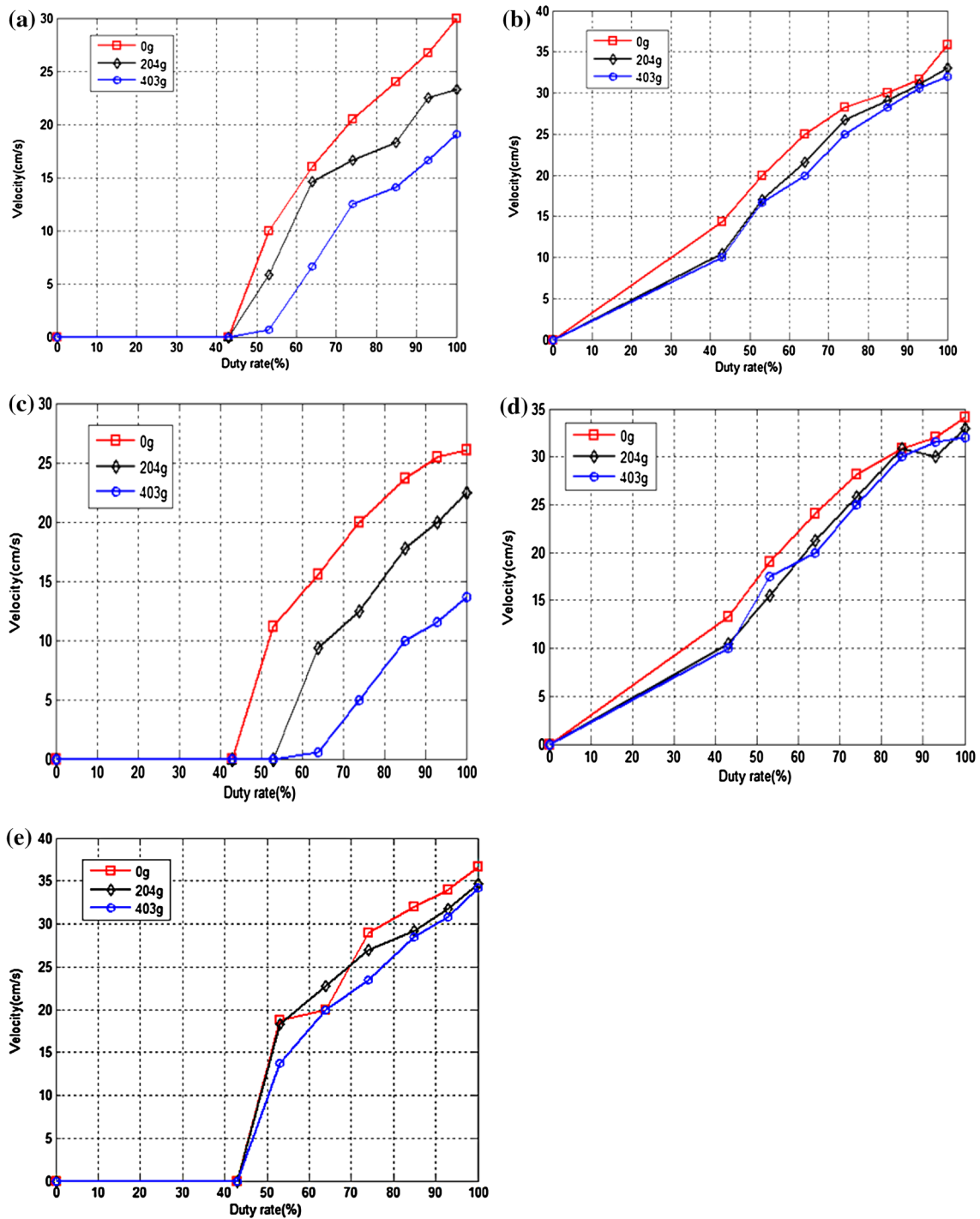


**Fig. 11** Results of crawling movement experiments on different terrains: **a** pavement, **b** asphalt road, **c** brick road, **d** cement floor, and **e** title floor

Figure 10 shows that without load, the maximum velocity of the robot is 8 cm/s at the frequency of 1.25 Hz on the title floor under quadruped movement pattern.

Figure 10 also shows that with the frequency increasing in less 1.25 Hz, the walk velocity of the robot increases

and when the frequency is more than 1.25 Hz, with the frequency increasing the walk velocity of the robot decreases. In the vicinity of the band 1.25 Hz, with the increase of load weight, the velocity of the robot has relatively large attenuation. Thus, increased load on the robot has more

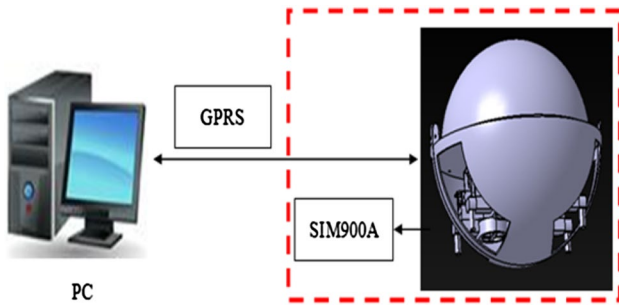


Fig. 12 The diagram of system structure

effect on movement velocity of the robot. However, in the low or high bands, increased load on the robot has less effect on movement velocity of the robot.

When the novel amphibious spherical robot walked in wheel movement gait, we can get the relationship figure between duty ratio and speed of the robot. It is shown in Fig. 11.

Figure 11 shows that without load, the maximum velocity of the robot is 36.7 cm/s at the duty of 100 % on the title floor under wheel movement pattern.

Figure 11 also shows that with the duty increasing, the walk velocity of the robot increases. With the increase of load weight, the velocity of the robot has relatively small attenuation. Thus, increased load on the robot has little effect on movement velocity of the robot.

Figures 10 and 11 show that in two movement patterns, robot moving speed decreases with the load increasing in the same terrain.

### 3.5 Localization experiment

Localization experiment of the robot was conducted. Figure 12 shows the diagram of system structure. The GPS data of the robot can be transmitted to the mobile terminal through the GPRS network. Mobile terminal is connected to the Internet. Finally, the data is transferred to the computer. We program on Labview software. GPS data can be displayed in the Labview. Figure 13 shows the figure of the robot's localization experiment. Figure 14 shows the front panel of the program on Labview. Figure 15 shows the program diagram on Labview.

## 4 Hydrodynamic analysis of the water-jet propeller

Underwater motions of the robot mainly rely on the four water-jet propellers, so it is necessary to measure relationship between actuating force of the water-jet propeller and the duty ratio. Hydrodynamic analysis of the water-jet propeller model requires three steps.



Fig. 13 The robot's localization experiment

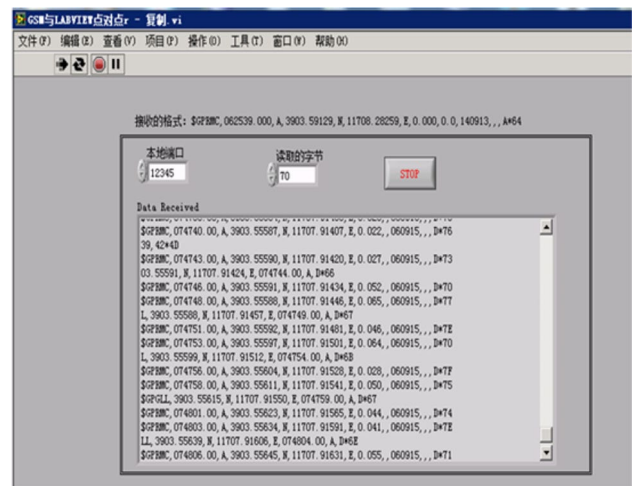


Fig. 14 The front panel of the program on Labview

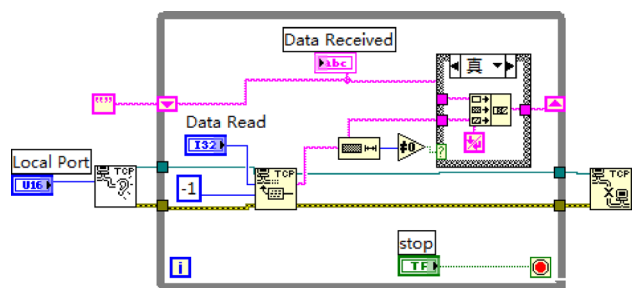


Fig. 15 The program diagram on Labview

- Step 1 Gambit software is employed to establish the 3D goal model. After considering the complexity of the model, we simplify them to some extent.
- Step 2 We use gambit software to divide the unstructured grid of the model.
- Step 3 Unstructured grid of the model is saved in.msh format and imported to the fluent software.

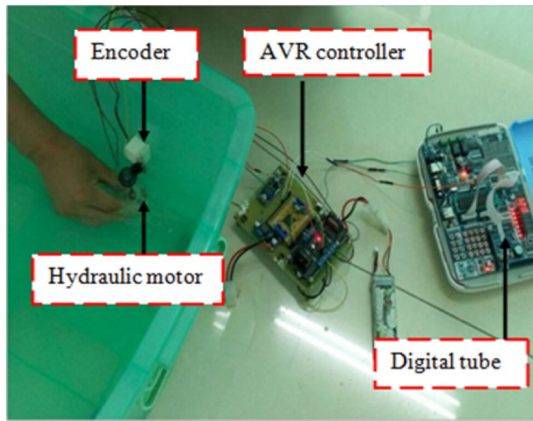


Fig. 16 The diagram of measuring relationship

The goal model is analyzed in fluid mechanics by fluent software. Before hydrodynamic analysis of the water-jet propeller model, we need to know the relationship between rotational speed of the *propeller of water-jet propeller* and the duty ratio.

#### 4.1 Relationship between rotational speed of the propeller of water-jet propeller and the duty ratio

Figure 16 shows the diagram of measuring relationship between Rotational speed of the water-jet propeller and the duty ratio. In order to the validity of the data, we put water-jet propeller in water. The AVR controller exports different duty ratio signals, which can drive the water-jet propeller rotation. Using photoelectric encoder reads pulse number. The final data results display in digital tube.

In order to ensure the effectiveness of the experiment data, all experiments were repeated several times to achieve an average rotational speed. Figure 17 shows the measuring results.

#### 4.2 Modeling of the water-jet propeller

Considering the problem of computer configuration and computing time, we have to simplify the model in a certain degree. Using Gambit software (2001) draws the simplified 3D model of the Water-jet propeller. Before meshing, we need to establish a cylinder flow field. The diameter and length of the cylinder are weighed. Several major issues are taken into account. Firstly, cylinder size doesn't have an adversely affect on the results of hydrodynamic analysis as far as possible; second, Considering configuration and computational speed of the computer, we don't adopt a large cylinder. The target model is shown in Fig. 18.

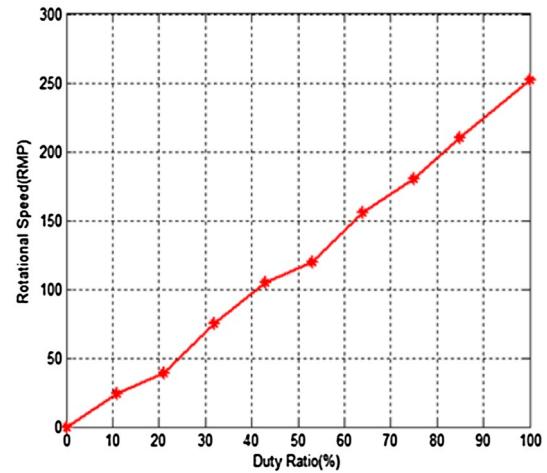


Fig. 17 The result of measuring relationship

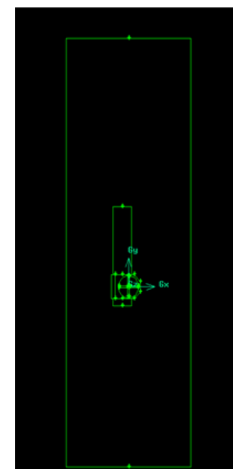


Fig. 18 Target model

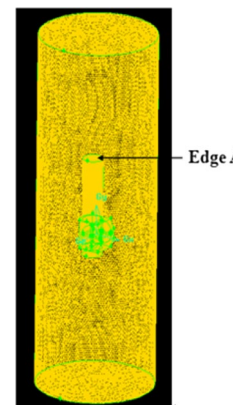


Fig. 19 Grid model

**Table 1** Details of the grid

Cells	Faces	Nodes	Partitions
1,956,031	3,966,155	353,056	1

### 4.3 Meshing of the water-jet propeller

Before hydrodynamic analysis of the model, meshing is a very important step. Based on the structure of the model, unstructured grids are put into use. Grid model is shown in Fig. 19. Finally, the file is saved in.msh format and imported to the fluent software.

The grid quality and the quantity are important in the fluid hydrodynamic analysis. In this paper, grid quantity is more than 1.9 million. The information of grid is as follows (Table 1).

### 4.4 Hydrodynamic analysis of the water-jet propeller

The finite volume based CFD software Fluent is used for the underwater motion simulation analysis by exploiting the turbulence model.

Before the simulation calculation, we need to set some conditions. For example, the boundary condition of inlet is set to velocity inlet; the boundary condition of outlet is set to pressure output. Pressure based solver and standard k-epsilon model are adopted to analyze goal model. In order to facilitate problem solving, we set a small cylinder which surround the propeller of water-jet propeller is rotating. We use the MRF model for simulation analysis (Fluent 2006).

After 750 times of calculation iteration, we get the residual error convergence curves. It is shown as Fig. 20. The figure shows that the simulation result is convergent. Velocity vector of the goal model and velocity magnitude of the goal model in XOY plane are respectively shown in Figs. 21 and 22.

Finally, we get Mass Flow Rate of the edge A. The data is shown as Table 2.

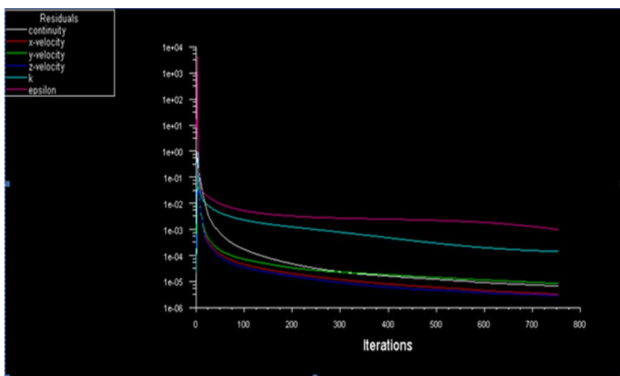


**Fig. 20** Residual error convergence curve

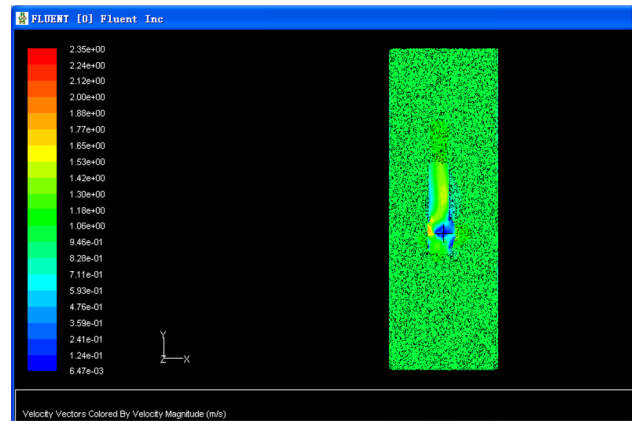


**Fig. 21** Velocity vector

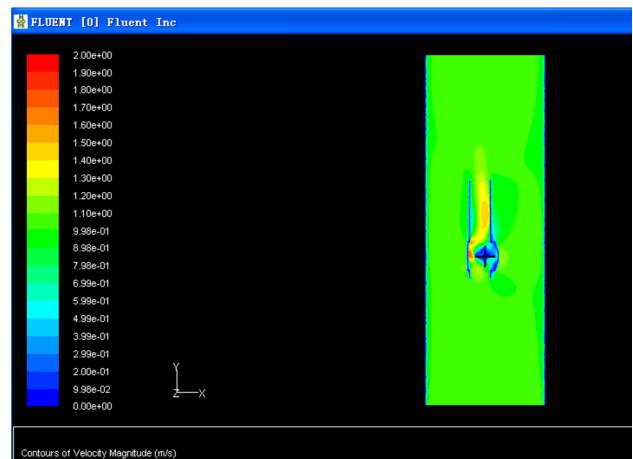


**Fig. 22** Velocity magnitude

By changing the value of a small cylinder rotation speed, we got the relationship between the rotational speed and Mass Flow Rate of the edge A. It is shown as Fig. 23.

As we know, the radius of the edge A is 0.006 m,  $\rho = 1000 \text{ L/m}^3$ .

$$Ft = mv \tag{1}$$

$$F = Mv \tag{2}$$

$$M = \rho sv \tag{3}$$

$$s = r^2 \tag{4}$$

**Table 2** Mass flow rate of the edge A

Mass flow rate	kg/s
A	0.096525863
Net	0.096525863

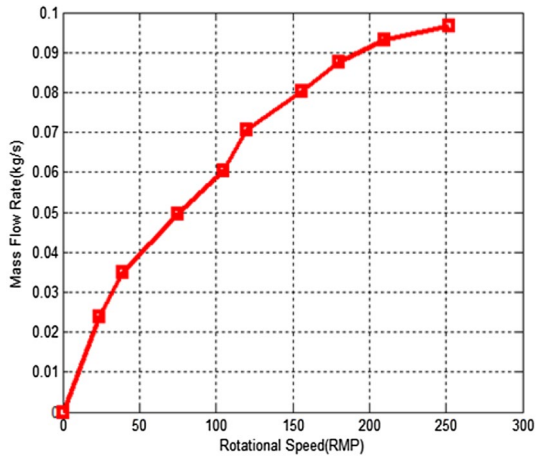


Fig. 23 The relationship between mass flow rate and the rotational speed

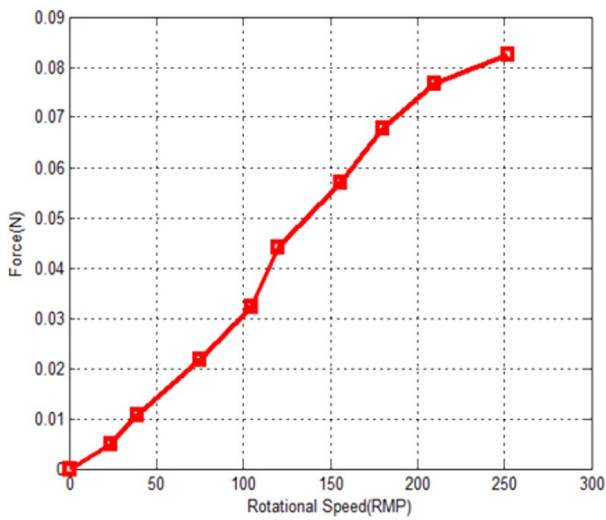


Fig. 24 The relationship between force and the rotational speed

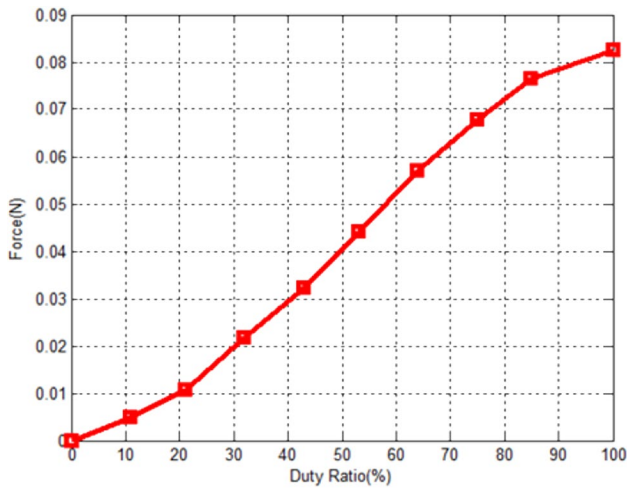


Fig. 25 The relationship between actuating force and the duty ratio

we can get

$$F = \frac{M^2}{0.11304} N \tag{5}$$

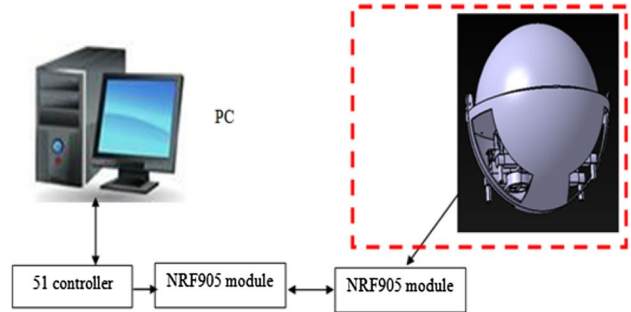


Fig. 26 The diagram of system structure

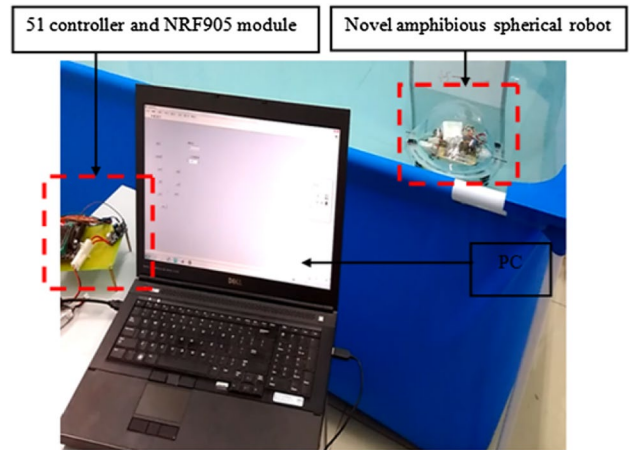


Fig. 27 The figure of the robot's wireless control experiment

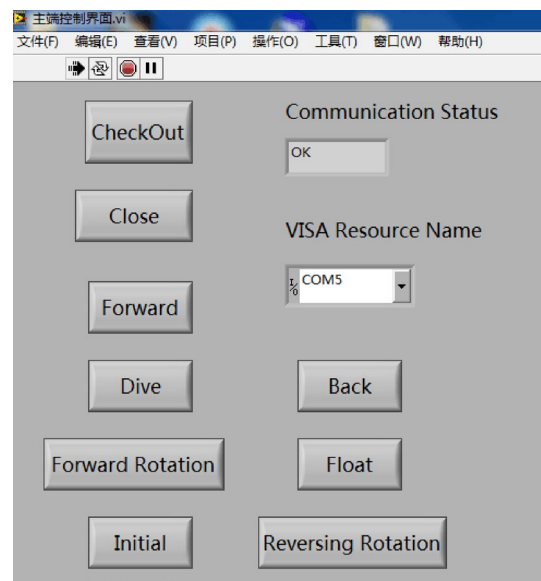


Fig. 28 The front panel of the program on labview

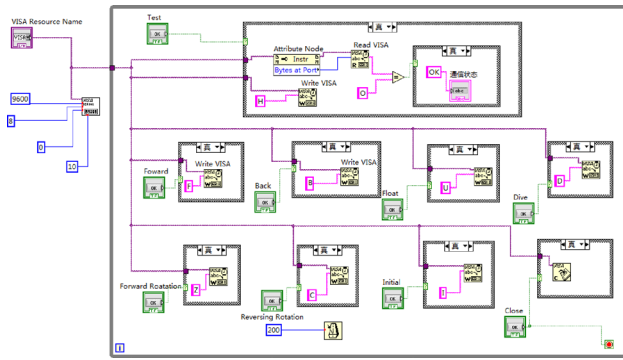
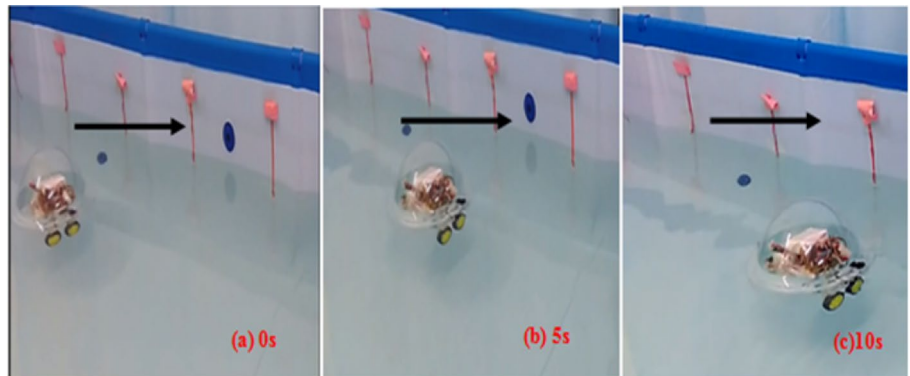


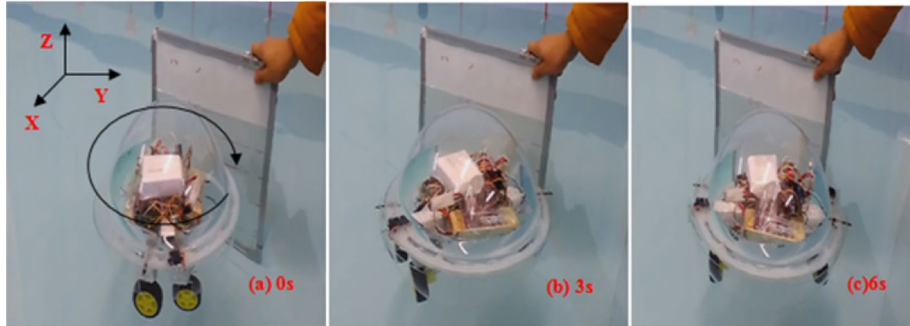
Fig. 29 The program diagram on labview

We got the relationship between the rotational speed and Force. It is shown as Fig. 24.

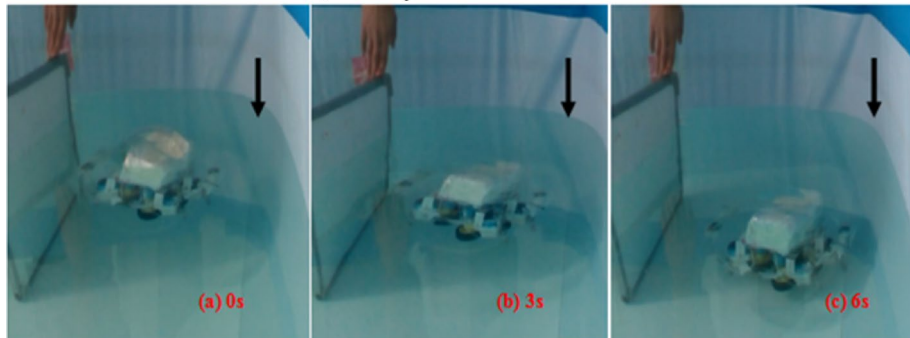
Fig. 30 Movement process of the robot



(a) Forward movement of the robot



(b) Rotary movement of the robot



(c) Dive movement of the robot

Finally, from Figs. 17 and 24, we got the relationship between actuating force of the water-jet propeller and the duty ratio. It is shown as Fig. 25.

### 5 Wireless control of the robot

In this paper, wireless control experiment of the robot was conducted. Figure 26 shows the diagram of system structure. In order to effectively control the robot freely switching movement pattern. We use NRF module for communication between the computer and the robot. We program on Labview software. Figure 27 shows the figure of the robot's wireless control experiment.

Figure 28 shows the front panel of the program on Labview. We use the mouse click on the button so that we can

control the robot to switch movement pattern. Figure 29 shows the Program diagram on Labview, Using the camera record the robot's movement in water, movement process of the robot are shown as Fig. 30.

The maximum forward speed of the novel spherical amphibious robot in water can reach 7.8 cm/s, the maximum rotary speed can reach 0.32 rad/s, the maximum dive speed can reach 6.2 cm/s. Experiments have also verified the wireless control system can realize the novel spherical amphibious robot switch freely movement in water.

## 6 Conclusions and future work

This paper proposed a new kind of the amphibious spherical robot. The robot can constitute three movement structure ways according to the environment, including wheel structure movement or quadruped walking movement adopted on land and water jet propulsion in water. According to different land conditions, there are two movement patterns to switch. While the ground is relatively flat, wheel structure pattern is adopted by the robot to improve movement speed. While the ground is more rigorous, the robot can use quadruped movement pattern to climb over obstacles. We carried out characteristic evaluation for the developed novel amphibious spherical robot in two movement patterns according to the condition of different terrains and different loads on land.

Hydrodynamic performance of the water-jet propeller model was analyzed. Gambit software is employed to establish and mesh the water-jet propeller model. Simulation analysis of the model is implemented by computational fluid dynamics (CFD) code, FLUENT software. In addition, the localization control and wireless control of the robot were conducted.

We can get some conclusions.

1. Without load, the maximum velocity of the robot is 8 cm/s at the frequency of 1.25 Hz on the title floor under quadruped movement pattern and the maximum velocity of the robot is 36.7 cm/s at the duty of 100 % on the title floor under wheel movement pattern.
2. Wheel movement improves movement speed of the amphibious spherical robot under the flat ground terrain.
3. The relationship between actuating force of the water-jet propeller and the duty ratio is obtained.
4. The maximum forward speed of the robot in water can reach 7.8 cm/s, the maximum rotary speed can reach 0.32 rad/s.

The maximum dive speed can reach 6.2 cm/s. Experimental results indicated that the developed novel amphibious spherical robot is feasible to develop marine resources and implement marine missions.

In future, in order to gather more information, sensors will be added to the robot. An advanced control algorithm will be applied to control the robot.

**Acknowledgments** This research is partly supported by National Natural Science Foundation of China (61375094), Key Research Program of the Natural Science Foundation of Tianjin (13JCZDJC26200), and National High Tech. Research and Development Program of China (2015AA043202).

## References

- Cai R, Chen Y, Lang L et al (2013) Inverse kinematics of a new quadruped robot control method. *Int J Adv Robot Syst* 10(46):1–8
- Dey BB, Manjanna S, Dudek G (2013) Ninja legs: amphibious one degree of freedom robotic legs. In: 2013 IEEE/RSJ international conference on intelligent robots and systems (IROS), pp 5622–5628
- Endo G, Hirose S (1999) Study on roller-walker. *IEEE Int Conf Robot Autom* 1:2032–2237
- FLUENT 6.3 User's Guide (2006) FLUENT Inc.
- GAMBIT 2 User's Guide (2001) FLUENT Inc.
- Guo S, Du J, Ye X et al (2010) Real-time adjusting control algorithm for the spherical underwater robot. *Information* 13(6):2021–2029
- Guo S, Du J, Ye X et al (2011) The computational design of a water jet propulsion spherical underwater vehicle. In: Proceedings of the 2011 IEEE international conference on mechatronics and automation, pp 2375–2379
- Guo S, Mao S, Shi L et al (2012a) Design and kinematic analysis of an amphibious spherical robot. In: Proceedings of the 2012 IEEE international conference on mechatronics and automation, pp 2214–2219
- Guo S, Shi L, Xiao N, Asaka K (2012b) A biomimetic underwater microrobot with multifunctional locomotion. *Robot Auton Syst* 60(12):1472–1483
- Guo S, Mao S, Shi L et al (2013) Development of an amphibious mother spherical robot used as the carrier for underwater microrobots. In: Proceedings of the 2012 ICME international conference on complex medical engineering, pp 758–762
- Halme A, Schonberg T, Wang Y (1996) Motion control of a spherical mobile robot. In: Proceedings of the 1996 4th international workshop on advanced motion control, Vol 1, pp 259–264
- He Y, Guo S, Shi L (2015) Preliminary mechanical analysis of an improved amphibious spherical father robot, *microsystem technologies* (in press)
- Kazemi H, Majd VJ et al (2013) Modeling and robust backstepping control of an underactuated quadruped robot in bounding motion. *Robotica* 31(03):423–439
- Lan X, Sun H, Jia Q (2010) Principle and dynamic analysis of a new-type spherical underwater vehicle. *J Beijing Univ Posts Telecommun* 33(3):20–23
- Li Y, Guo S, Yue C (2015a) Preliminary concept of a novel spherical underwater robot. *Int J Mechatron Autom* 5(1):11–21
- Li M, Guo S, Hirata H, Ishihara H (2015b) Design and performance evaluation of an amphibious spherical robot. *Robot Auton Syst* 64:21–34

- Lin X, Guo S, Yue C et al (2013) 3D modelling of a vectored water jet-based multi-propeller propulsion system for a spherical underwater robot. *Int J Adv Rob Syst* 10(80):1–8
- Loc V-G, Koo IM, Tran DT et al (2012) Body workspace of quadruped walking robot and its applicability in legged locomotion. *J Intell Robot Syst* 67(3–4):271–284
- Marani G, Choi SK, Yuh J (2009) Underwater autonomous manipulation for intervention missions AUVs. *Ocean Eng* 36(1):15–23
- Mazumdar A, Asada HH (2011) A compact underwater vehicle using high-bandwidth coanda-effect valves for low speed precision maneuvering in cluttered environments. In: *IEEE international conference on robotics and automation*, pp 1544–1550
- Mazumdar A, Asada HH (2013) Pulse width modulation of water jet propulsion systems using high-speed coanda-effect valves. *J Dyn Syst Meas Contr* 135:051019
- Mazumdar A, Lozano M, Fittery A, Asada HH (2012) A compact, manoeuvrable, underwater robot for direct inspection of nuclear power piping systems. In: *IEEE international conference on robotics and automation*, pp 2818–2823
- Mazumdar A, Fittery A, Ubellacker W, Asada HH (2013) A ball-shaped underwater robot for direct inspection of nuclear reactors and other water-filled infrastructure. In: *IEEE international conference on robotics and automation*, pp 3400–3407
- Pan S, Shi L, Guo S (2015) A kinect-based real-time compressive tracking prototype system for amphibious spherical robots. *Sensors* 15(4):8232–8252
- Ryuha Y-S, Yanga G-H, Liu J, Huo H (2015) A school of robotic fish for mariculture monitoring in the sea coast. *J Bionic Eng* 12(1):37–46
- Saout O, Ananthakrishnan P (2011) Hydrodynamic and dynamic analysis to determine the directional stability of an underwater vehicle near a free surface. *Appl Ocean Res* 33(2):158–167
- Shen S-Y, Li C-H, Cheng C-C et al. (2009) Design of a leg-wheel hybrid mobile platform. In: *The 2009 IEEE/RSJ international conference on intelligent robots and systems*, pp 4682–4687
- Shi L, Guo S, Asaka K (2011) A bio-inspired underwater microrobot with compact structure and multifunctional locomotion. In: *Proceedings of IEEE/ASME international conference on advanced intelligent mechatronics*, pp 203–208
- Shi L, Guo S, Mao S (2013) Development of an amphibious turtle-inspired spherical mother robot. *J Bionic Eng* 10(4):446–455
- Ting MC, Abdul Mujeebu M, Abdullah MZ, Arshad MR (2012) Numerical study on hydrodynamic performance of shallow underwater glider platform. *Indian J Geo Mar Sci* 41(2):124–133
- Wan F, Guo S, Ma X et al. (2014) Characteristic analysis on land for an amphibious spherical robot. In: *Proceedings of 2014 IEEE international conference on mechatronics and automation*, pp 1945–1950
- Watson SA, Crutchley DJP, Green PN (2012) The mechatronic design of a micro-autonomous underwater vehicle ( $\mu$ AUV). *Mechatron Autom* 2(3):157–168
- Yue C, Guo S, Shi L (2013a) Hydrodynamic analysis of the spherical underwater robot SUR-II. *Int J Adv Rob Syst* 10:1–12
- Yue C, Guo S, Li M (2013) ANSYS FLUENT-based modeling and hydrodynamic analysis for a spherical underwater robot. In: *Proceedings of 2013 IEEE international conference on mechatronics and automation*, pp 1577–1581
- Yue C, Guo S, Li M et al (2015) Mechatronic system and experiments of a spherical underwater robot: SUR-II. *J Intell Robot Syst* (**in press**)
- Yue C, Guo S, Shi L (2015) Design and performance evaluation of a biomimetic microrobot for the father–son underwater intervention robotic system. *Microsystem Technologies* (**in press**)
- Yue C, Guo S, Li M (2015) Characteristics evaluation of a biomimetic microrobot for a father-son underwater intervention robotic system. In: *2015 IEEE/RSJ international conference on intelligent robots and systems (IROS)*, pp 171–176